

Methods

TiO₂ nanotube fabrication. TiO₂ nanotube arrays were formed via anodic oxidation in an electrolytic solution containing 0.2M Sodium Citrate Tribasic, 1M Sodium Hydrogen Sulfate, and 0.1M Potassium Fluoride, with Sodium Hydroxide added to adjust the pH of the solution. Titanium foil (0.25mm thick, 99.7% purity, Alfa Aesar) were anodized at a constant DC potential for 17 hours in a two-electrode electrochemical cell with a platinum foil as the counter electrode. The average length and pore diameter of the nanotubes were scaled by varying the pH of the electrolyte and the DC potential during anodization. Nanotubes 1 μm in length with an average pore diameter of 30 nm were prepared by anodization using 10 V bias in the 4 pH electrolyte. Nanotubes 1 μm in length with an average pore diameter of 100 nm were prepared by anodization using 20 V bias in a 2 pH electrolyte. All samples were subsequently rinsed in DI water and annealed at a temperature of 500 °C in oxygen ambient to crystallize the nanotubes. Heating and cooling rates of 1 °C/min were used with a dwell time of 6 hours. Surfaces were sterilized with 70% ethanol and UV prior to use in tissue culture.

HAEC and HAoSMC culture. Primary human aortic endothelial cells (HAECs) and primary human vascular smooth muscle cells (HAoSMCs) (Lonza, Walkersville, MD) were cultured according to manufacturer's instructions using Lonza's HAEC and HAoSMC complete media. The cells were cultured in a humidified 95% air/5% CO₂ incubator at 37°C. Cells used in this experiment were passaged less than 15 times.

RNA isolation for microarray. HAECs and HAoSMCs were seeded at 5 x 10⁴ cells/cm² on flat and nanotube substrates. Cells were harvested after 24 hours using Qiagen's RNeasy kit (Valencia, CA) according to manufacturer's instructions. Concentration and purity of isolated RNA was measured using a NanoDrop spectrophotometer (Thermo Fisher Scientific, Wilmington, DE)

Microarray. Sample preparation, labeling, and array hybridizations were performed according to standard protocols from the UCSF Shared Microarray Core Facilities and Agilent Technologies (<http://www.arrays.ucsf.edu> and <http://www.agilent.com>). Total RNA quality was assessed using a Pico Chip on an Agilent 2100 Bioanalyzer (Agilent Technologies, Palo Alto, CA). RNA was amplified and labeled with Cy3-CTP using the Agilent low RNA input fluorescent linear amplification kits following the manufacturers protocol. Labeled cRNA was assessed using the Nanodrop ND-100 (Thermo Fisher Scientific), and equal amounts of Cy3 labeled target were hybridized to Agilent whole human genome 4x44K Ink-jet arrays. Hybridizations were performed for 14 hrs, according to the manufacturer's protocol. Arrays were scanned using the Agilent microarray scanner and raw signal intensities were extracted with Feature Extraction v10.1 software. A total of 19 arrays were hybridized and represent 4 biological replicates for each group (with the exception of group VSMC-NT30, which has 3 biological replicates).

Differential expression analysis. The following terminology is used to discuss the results of our analysis:

M – $\log_2 (S2/S1)$. Log 2 based fold change of entity of interest. M=1 means two-fold increase in S2 compared to S1. M=0 means equal expression. M=-1 means 2 fold down-regulation.

aveA—average \log_2 based intensity of the same probe across all arrays, a proxy for gene expression level

B - log posterior odds ratios, ratio between the probability that a given gene is **differentially expressed (DE)** over the probability that a given gene is not differentially expressed; $B \geq 0$ means equal or more probability that a gene is DE than non-DE.¹

FDR – False Discovery Rate, which is the percentage of falsely declared DE genes among the set of declared DE genes. A FDR cutoff of 0.01 indicates that 1% of the declared DE genes are expected to false positives.²

AdjP – Adjusted p-value, which controls for family-wise error rates, the probability of having more than one false discovery. An adjusted p-value cutoff of 0.01 indicates that the declared DE set has 1% chance to have more than one false positive.

Raw log-intensities are normalized using *quantile* normalization method that is proposed by Bolstad *et al.*³ No background subtraction was performed, and the median feature pixel intensity was used as the raw signal before normalization.

A one-way ANOVA model is formulated and specific contrasts are formulated to examine the two pairwise comparisons of interest. Moderated t-statistic, B statistic, false discovery rate and p-value for each gene were obtained. Adjusted p-values were produced by the method proposed by Holm.⁴ All procedures were carried out using functions in the R package *limma* in *Bioconductor*.^{5,6} Shortlists for HAECs were generated using the criteria of $B \geq 0$ and Nominal $P \leq 0.001$. Shortlists for HAoSMCs were generated using the criteria of $B > 0$, Nominal $P \leq 0.001$, and fold-change > 2 (i.e. absolute value of \log_2 fold-change > 1).

Quantitative Polymerase Chain Reaction. For confirmation of microarray data, cells were seeded at 5×10^4 cells/cm² on flat and nanotube surfaces. In addition, ECs were also seeded at 5×10^3 cells/cm² for low density experiments. After 24 hours, samples were harvested using Ambion/Applied Biosystems's Cell to C_T kit (Foster City, CA). Lysis, RT-PCR, and qPCR were performed according to manufacturer's instructions using a StepOne Plus instrument (Applied Biosystems). Primers for each target were designed by Primer Express 3.0 software (Applied Biosystems) or obtained from the National Cancer Institute's Quantitative PCR Primer Database (<http://web.ncifcrf.gov/rtp/gel/primerdb/>) for the following genes: FST (forward primer – 5'-CAGTAAGTCGGATGAGCCTGTCT, reverse primer – 5'-CAGCTTCCTTCATGGCACACT), ATF3 (forward – 5'-CTGCCCCGCCTTTCATCTG,

reverse – 5'-CAGACACTGCTGCCTGAATCC), EGR1 (forward – 5'-TTTGCCAGGAGCGATGAAC, reverse – 5'-CCGAAGAGGCCACAACACTT), YAP1 (forward – 5'-CGTCCAGCAAGATACTTTAATCCTCTAT, reverse – 5'-CTGTGAAAGAGGTCAGCAATACATT), and GAPDH (forward – 5'-TGCACCACCAACTGCTTAGC, reverse – 5'-GGCATGGACTGTGGTCATGAG). Each experimental condition was performed three times (n=3). Expression levels of the genes were measured in technical triplicates.

Supplemental Information

Microarray data has been submitted to the GEO (accession number: GSE17676) and can be found at the following address:

<http://www.ncbi.nlm.nih.gov/geo/query/acc.cgi?token=zhinfukqcyiqebk&acc=GSE17676>

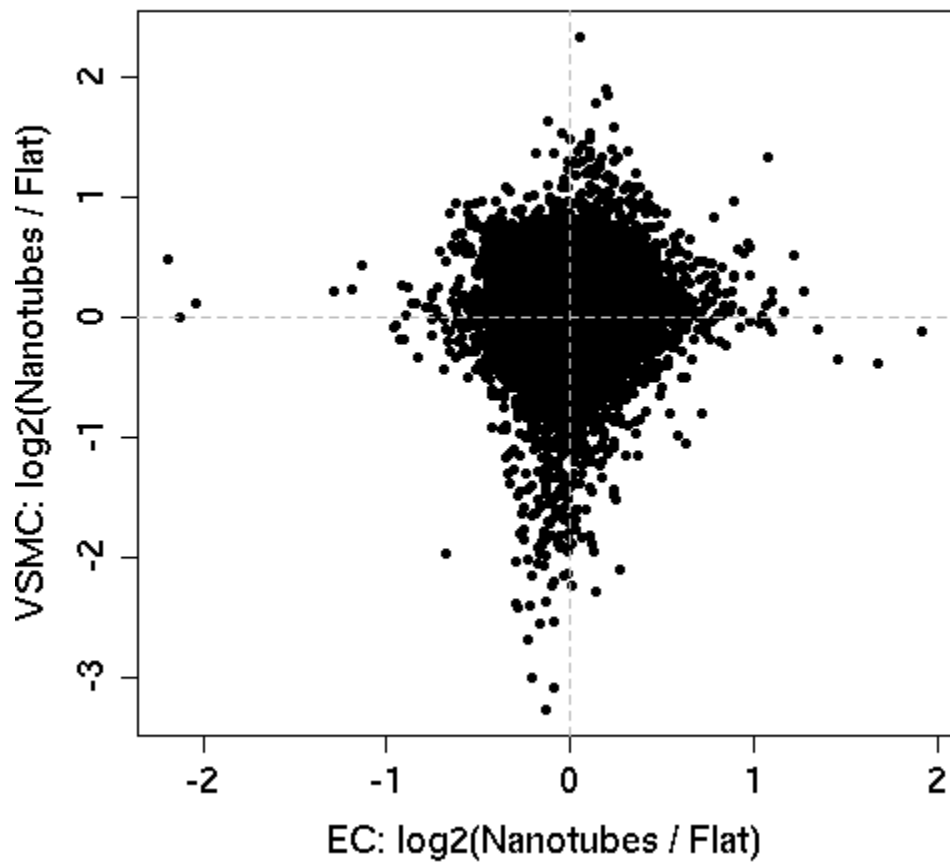
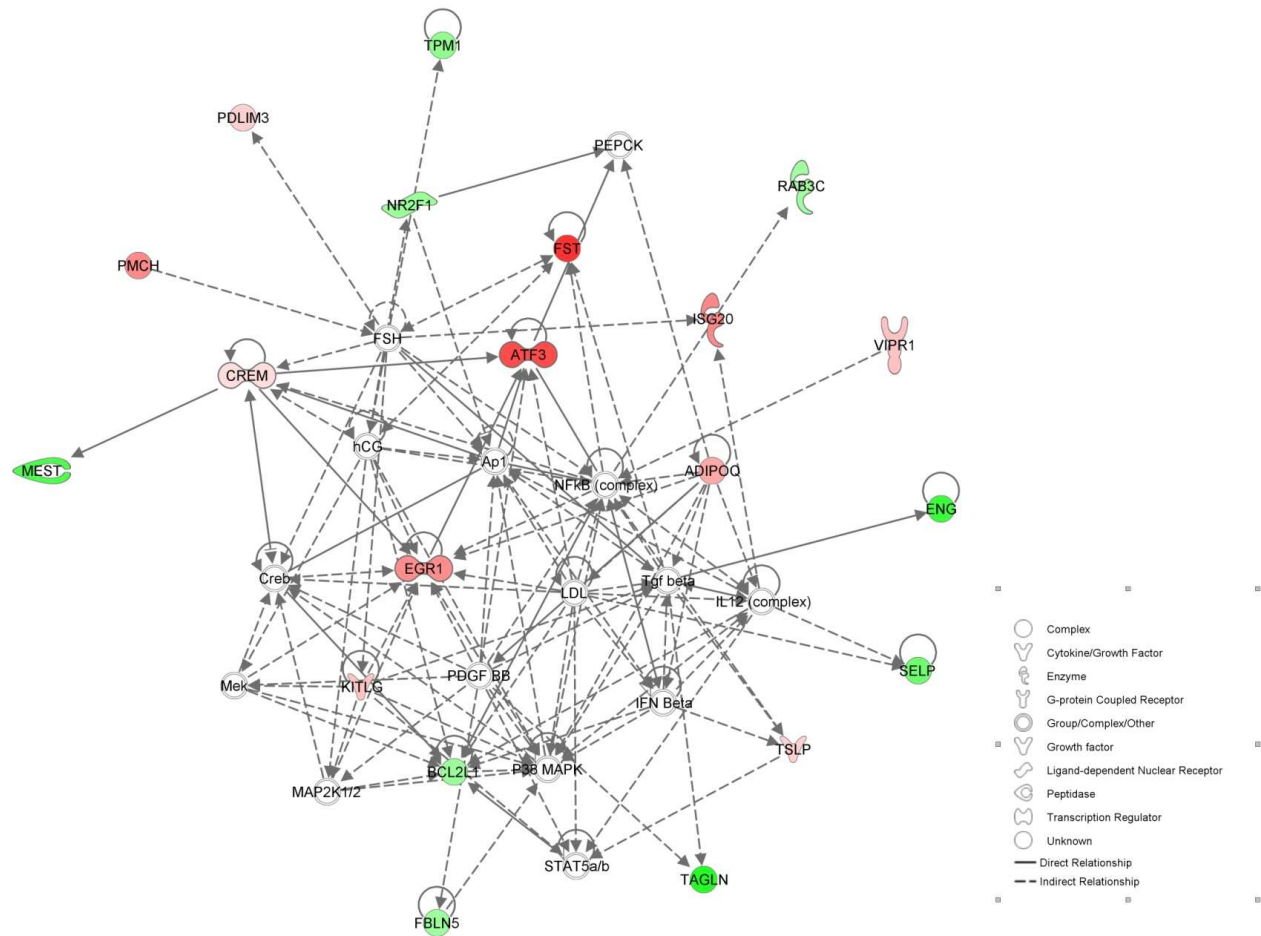
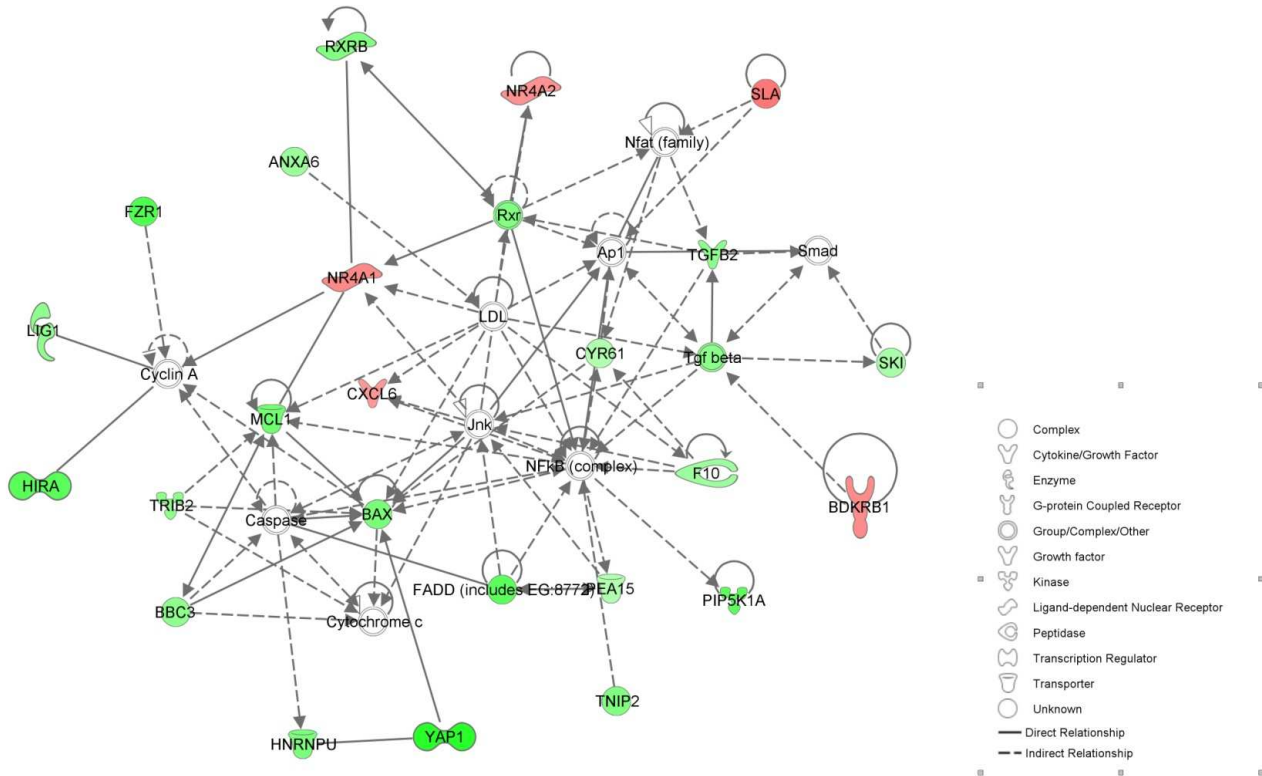


Figure S1: MM plot of gene expression for VSMCs vs. ECs.



© 2000-2009 Ingenuity Systems, Inc. All rights reserved.

Figure S2. Original top network plot for ECs generated by Ingenuity Pathway Analysis. Red indicates upregulation, green down regulation. Intensity of color is proportional to magnitude of change.



© 2000-2009 Ingenuity Systems, Inc. All rights reserved.

Figure S3. Original top network plot for VSMCs generated by Ingenuity Pathway Analysis. Red indicates upregulation, green down regulation. Intensity of color is proportional to magnitude of change.

Table S1: Genes significantly affected by exposure to nanotubes are listed according to their affect on a specific process. Those that have been shown in literature to inhibit a process are listed on the left two columns, and those that promote the process are listed on the right columns. Superscript refers to literature identified through IPA's curated findings that support all of the gene's classification(s). Data from these tables were used to plot Figures 1B and 4B.

A. Human Aortic Endothelial Cells

Proliferation/Cell Cycle Progression

Inhibit	log2FC.NTvsTi	Promote	log2FC.NTvsTi
CCL23 ^{7, 8}	-0.84	ENG ^{9, 10}	-0.83
TPM1 ^{11, 12}	-0.47	RPS15A ¹³	-0.33
FBLN5 ¹⁴	-0.41	TNS3 ¹⁵	0.34
CAPRIN2 ¹⁶	-0.19	CREM ¹⁷	0.3
PFDN5 ¹⁸	-0.32	TSLP ¹⁹⁻²¹	0.43
NOV ²²	0.6	KITLG ²³⁻²⁵	0.54
GPR68 ²⁶	0.63	VIPR1 ²⁷	0.56
ADIPOQ ²⁸⁻³⁰	0.8	TNXB ^{31, 32}	0.55
		ISG20 ³³	1.1
		EGR1 ^{34, 35}	1.04
		ATF3 ^{36, 37}	1.67
		FST ³⁸	1.91

Migration

Inhibit	log2FC.NTvsTi	Promote	log2FC.NTvsTi
ENG ^{9, 10}	-0.83	TPM1 ^{11, 12}	-0.47
		FBLN5 ¹⁴	-0.41
		KITLG ²³⁻²⁵	0.54

		MFI2 ³⁹	0.6
		NOV ²²	0.6
		ADIPOQ ²⁸⁻³⁰	0.8
		CCR3 ⁴⁰	1.03
		FST ³⁸	1.91

Inflammation/Coagulation

Inhibit	log2FC.NTvsTi	Promote	log2FC.NTvsTi
KITLG ²³⁻²⁵	0.54	CCL23 ^{7, 8}	-0.84
TNXB ^{31, 32}	0.55	SELP ⁴¹	-0.61
		GPR4 ^{42, 43}	-0.49
		IL13RA1 ⁴⁴	-0.34
		TSLP ¹⁹⁻²¹	0.43

Apoptosis/Cell Death

Inhibit	log2FC.NTvsTi	Promote	log2FC.NTvsTi
NR2F1 ⁴⁵	-0.42	CAPRIN2 ¹⁶	-0.19
GPX3 ⁴⁶	0.34	ITPR3 ⁴⁷	0.44
TSLP ¹⁹⁻²¹	0.43	CREM ¹⁷	0.3
NEK8 ⁴⁸	0.67		
ADIPOQ ²⁸⁻³⁰	0.8		
SLC12A2 ⁴⁹	0.72		
PPID ^{40, 50}	0.84		
EGR1 ^{34, 35}	1.04		
ATF3 ^{36, 37}	1.67		

B. Human Aortic Vascular Smooth Muscle Cells

Proliferation/Cell Cycle Progression

Inhibit	log2FC.NTvsTi	Promote	log2FC.NTvsTi
HIRA ⁵¹	-2.4	YAP1 ^{52, 53}	-3.09
IGF2R ^{54, 55}	-1.83	FADD ^{56, 57}	-2.38
VPS18 ⁵⁸	-1.6	PRPF19 ⁵⁹	-2.15
KCTD11 ⁶⁰	-1.43	GBF1 ⁶¹	-2.13
ATF5 ^{62, 63}	-1.36	MCL1 ^{64, 65}	-2.07
HMOX1 ^{66, 67}	-1.06	FUS ^{68, 69}	-2.04
EREG ^{70, 71}	1.02	RALGDS ^{72, 73}	-2.02
BDKRB2 ^{74, 75}	1.17	H19 ⁷⁶	-1.92
NR4A2 ^{77, 78}	1.22	IGF2R ^{54, 55}	-1.83
BDKRB1 ^{75, 79, 80}	1.3	SFRS5 ^{81, 82}	-1.82
NR4A1 ^{83, 84}	1.33	RXR ⁸⁵⁻⁸⁷	-1.81
SLA ^{88, 89}	1.53	TGFB2 ^{90, 91}	-1.67
		LIG1 ⁹²	-1.61
		SEMA4C ⁹³	-1.56
		F10 ^{94, 95}	-1.42
		NCL ⁹⁶	-1.42
		ARRB1 ^{97, 98}	-1.32
		PPP1R8 ⁹⁹	-1.26
		THG1L ¹⁰⁰	-1.26
		RCC1 ¹⁰¹	-1.25
		SKI ^{102, 103}	-1.25
		ITGA2 ¹⁰⁴	-1.2
		PEA15 ^{105, 106}	-1.12
		CYR61 ¹⁰⁷	-1.12
		EWSR1 ¹⁰⁸	-1.1

		RBBP6 ¹⁰⁹	-1.08
		WASF2 ¹¹⁰	-1.02
		EREG ^{70, 71}	1.02

Migration

Inhibit	log2FC.NTvsTi	Promote	log2FC.NTvsTi
ABHD2 ¹¹¹	-1.95	PRKAG1 ²⁹	-2.69
TMBIM1 ¹¹²	-1.21	HNRPAB ¹¹³	-2.15
SOCS3 ^{114, 115}	-1.01	SEMA4C ⁹³	-1.56
		ARRB1 ^{97, 98}	-1.32
		PDLIM2 ¹¹⁶	-1.23
		ITGA2 ¹⁰⁴	-1.2
		WASF2 ¹¹⁰	-1.02
		MYO10 ¹¹⁷	-1.01
		CD151 ¹¹⁸	-1
		BDKRB1 ^{75, 79, 80}	1.29
		HAS1 ¹¹⁹	1.36
		IRS2 ¹²⁰	2.32

Inflammation/Coagulation

Inhibit	log2FC.NTvsTi	Promote	log2FC.NTvsTi
EXT1 ¹²¹	-1.16	LAMP1 ^{122, 123}	-2.23
ADAMTS13 ¹²⁴	1.2	RALGDS ^{72, 73}	-2.02
GLIS2 ¹²⁵	1.52	PEAR1 ¹²⁶	-1.8
SLA ^{88, 89}	1.53	ATRN ¹²⁷	-1.63
		CHST2 ¹²⁸	-1.58
		F10 ^{94, 95}	-1.42
		CXCL6 ¹²⁹	1.16
		BDKRB1 ^{75, 79, 80}	1.3

Apoptosis/Cell Death

Inhibit	log2FC.NTvsTi	Promote	log2FC.NTvsTi
YAP1 ^{52, 53}	-3.09	FADD ^{56, 57}	-2.38
PRPF19 ⁵⁹	-2.15	LAMP1 ^{122, 123}	-2.23
MCL1 ^{64, 65}	-2.07	AQP3 ¹³⁰	-2.1
SFRS5 ^{81, 82}	-1.82	FUS ^{68, 69}	-2.04
RXRβ ⁸⁵⁻⁸⁷	-1.81	BAX ¹³¹	-1.92
TNIP2 ¹³²	-1.81	IGF2R ^{54, 55}	-1.83

DNAJB2 ¹³³	-1.72	TRIB2 ¹³⁴	-1.67
ATF5 ^{62, 63}	-1.36	BBC3 ¹³⁵	-1.61
THG1L ¹⁰⁰	-1.26	UACA ¹³⁶	-1.49
SKI ^{102, 103}	-1.25	NCL ⁹⁶	-1.42
PEA15 ^{105, 106}	-1.12	TNKS2 ¹³⁷	-1.31
RBBP6 ¹⁰⁹	-1.08	SDHC ¹³⁸	-1.17
HMOX1	-1.06	SOCS3 ^{114, 115}	-1.01
BDKRB2 ^{74, 75}	1.17	NR4A1 ^{83, 84}	1.33
NR4A2 ^{77, 78}	1.22		
BDKRB1 ^{75, 79, 80}	1.29		
IRS2 ¹²⁰	2.32		

1. Lonnstedt, I. & Speed, T. Replicated microarray data. *Statistica Sinica* **12**, 31-46 (2002).
2. Benjamini, Y. & Hochberg, Y. Controlling the False Discovery Rate - a Practical and Powerful Approach to Multiple Testing. *Journal of the Royal Statistical Society Series B-Methodological* **57**, 289-300 (1995).
3. Bolstad, B.M., Irizarry, R.A., Astrand, M. & Speed, T.P. A comparison of normalization methods for high density oligonucleotide array data based on variance and bias. *Bioinformatics* **19**, 185-193 (2003).
4. Holm, S. A simple sequentially rejective multiple test procedure. *Scandinavian Journal of Statistics*, 65-70 (1979).
5. Smyth, G.K. Linear models and empirical bayes methods for assessing differential expression in microarray experiments. *Stat Appl Genet Mol Biol* **3**, Article3 (2004).
6. Gentleman, R.C. et al. Bioconductor: open software development for computational biology and bioinformatics. *Genome Biol* **5**, R80 (2004).
7. Patel, V.P. et al. Molecular and functional characterization of two novel human C-C chemokines as inhibitors of two distinct classes of myeloid progenitors. *J Exp Med* **185**, 1163-1172 (1997).
8. Youn, B.S. et al. Characterization of CKbeta8 and CKbeta8-1: two alternatively spliced forms of human beta-chemokine, chemoattractants for neutrophils, monocytes, and lymphocytes, and potent agonists at CC chemokine receptor 1. *Blood* **91**, 3118-3126 (1998).
9. Lebrin, F. et al. Endoglin promotes endothelial cell proliferation and TGF-beta/ALK1 signal transduction. *Embo Journal* **23**, 4018-4028 (2004).
10. Liu, Y.Q., Jovanovic, B., Pins, M., Lee, C. & Bergan, R.C. Over expression of endoglin in human prostate cancer suppresses cell detachment, migration and invasion. *Oncogene* **21**, 8272-8281 (2002).
11. Zhu, S., Si, M.L., Wu, H. & Mo, Y.Y. MicroRNA-21 targets the tumor suppressor gene tropomyosin 1 (TPM1). *J Biol Chem* **282**, 14328-14336 (2007).
12. Bryce, N.S. et al. Specification of actin filament function and molecular composition by tropomyosin isoforms. *Mol Biol Cell* **14**, 1002-1016 (2003).

13. Lian, Z. et al. Human S15a expression is upregulated by hepatitis B virus X protein. *Mol Carcinog* **40**, 34-46 (2004).
14. Spencer, J.A. et al. Altered vascular remodeling in fibulin-5-deficient mice reveals a role of fibulin-5 in smooth muscle cell proliferation and migration. *Proc Natl Acad Sci U S A* **102**, 2946-2951 (2005).
15. Chiang, M.K., Liao, Y.C., Kuwabara, Y. & Lo, S.H. Inactivation of tensin3 in mice results in growth retardation and postnatal lethality. *Dev Biol* **279**, 368-377 (2005).
16. Aerbajinai, W., Lee, Y.T., Wojda, U., Barr, V.A. & Miller, J.L. Cloning and characterization of a gene expressed during terminal differentiation that encodes a novel inhibitor of growth. *J Biol Chem* **279**, 1916-1921 (2004).
17. Ding, B. et al. A positive feedback loop of phosphodiesterase 3 (PDE3) and inducible cAMP early repressor (ICER) leads to cardiomyocyte apoptosis. *Proc Natl Acad Sci U S A* **102**, 14771-14776 (2005).
18. Fujioka, Y. et al. MM-1, a c-Myc-binding protein, is a candidate for a tumor suppressor in leukemia/lymphoma and tongue cancer. *J Biol Chem* **276**, 45137-45144 (2001).
19. Pandey, A. et al. Cloning of a receptor subunit required for signaling by thymic stromal lymphopoietin. *Nat Immunol* **1**, 59-64 (2000).
20. Zhou, B. et al. Thymic stromal lymphopoietin as a key initiator of allergic airway inflammation in mice. *Nat Immunol* **6**, 1047-1053 (2005).
21. Brown, V.I. et al. Thymic stromal-derived lymphopoietin induces proliferation of pre-B leukemia and antagonizes mTOR inhibitors, suggesting a role for interleukin-7/Ralpha signaling. *Cancer Res* **67**, 9963-9970 (2007).
22. Benini, S. et al. In Ewing's sarcoma CCN3(NOV) inhibits proliferation while promoting migration and invasion of the same cell type. *Oncogene* **24**, 4349-4361 (2005).
23. Sawai, N. et al. Thrombopoietin augments stem cell factor-dependent growth of human mast cells from bone marrow multipotential hematopoietic progenitors. *Blood* **93**, 3703-3712 (1999).
24. Landuzzi, L. et al. The metastatic ability of Ewing's sarcoma cells is modulated by stem cell factor and by its receptor c-kit. *Am J Pathol* **157**, 2123-2131 (2000).
25. Sawada, J. et al. Stem cell factor has a suppressive activity to IgE-mediated chemotaxis of mast cells. *J Immunol* **174**, 3626-3632 (2005).
26. Xu, Y. et al. Sphingosylphosphorylcholine is a ligand for ovarian cancer G-protein-coupled receptor 1. *Nat Cell Biol* **2**, 261-267 (2000).
27. Moody, T.W. et al. A vasoactive intestinal peptide antagonist inhibits non-small cell lung cancer growth. *Proc Natl Acad Sci U S A* **90**, 4345-4349 (1993).
28. Arita, Y. et al. Adipocyte-derived plasma protein adiponectin acts as a platelet-derived growth factor-BB-binding protein and regulates growth factor-induced common postreceptor signal in vascular smooth muscle cell. *Circulation* **105**, 2893-2898 (2002).
29. Ouchi, N. et al. Adiponectin stimulates angiogenesis by promoting cross-talk between AMP-activated protein kinase and Akt signaling in endothelial cells. *J Biol Chem* **279**, 1304-1309 (2004).
30. Chandrasekar, B. et al. Adiponectin blocks interleukin-18-mediated endothelial cell death via APPL1-dependent AMP-activated protein kinase (AMPK) activation and IKK/NF-kappaB/PTEN suppression. *J Biol Chem* **283**, 24889-24898 (2008).
31. Loike, J.D., Cao, L., Budhu, S., Hoffman, S. & Silverstein, S.C. Blockade of alpha 5 beta 1 integrins reverses the inhibitory effect of tenascin on chemotaxis of human monocytes and polymorphonuclear leukocytes through three-dimensional gels of extracellular matrix proteins. *J Immunol* **166**, 7534-7542 (2001).
32. Scaffidi, A.K. et al. alpha(v)beta(3) Integrin interacts with the transforming growth factor beta (TGFbeta) type II receptor to potentiate the proliferative effects of TGFbeta1 in living human lung fibroblasts. *J Biol Chem* **279**, 37726-37733 (2004).

33. Lee, R.W. et al. CD4+CD25(int) T cells in inflammatory diseases refractory to treatment with glucocorticoids. *J Immunol* **179**, 7941-7948 (2007).
34. Baron, V. et al. Inhibition of Egr-1 expression reverses transformation of prostate cancer cells in vitro and in vivo. *Oncogene* **22**, 4194-4204 (2003).
35. Weisz, L. et al. Transactivation of the EGR1 gene contributes to mutant p53 gain of function. *Cancer Res* **64**, 8318-8327 (2004).
36. Perez, S., Vial, E., van Dam, H. & Castellazzi, M. Transcription factor ATF3 partially transforms chick embryo fibroblasts by promoting growth factor-independent proliferation. *Oncogene* **20**, 1135-1141 (2001).
37. Kawauchi, J. et al. Transcriptional repressor activating transcription factor 3 protects human umbilical vein endothelial cells from tumor necrosis factor-alpha-induced apoptosis through down-regulation of p53 transcription. *J Biol Chem* **277**, 39025-39034 (2002).
38. Kozian, D.H., Ziche, M. & Augustin, H.G. The activin-binding protein follistatin regulates autocrine endothelial cell activity and induces angiogenesis. *Lab Invest* **76**, 267-276 (1997).
39. Demeule, M. et al. Regulation of plasminogen activation: a role for melanotransferrin (p97) in cell migration. *Blood* **102**, 1723-1731 (2003).
40. Salcedo, R. et al. Eotaxin (CCL11) induces in vivo angiogenic responses by human CCR3+ endothelial cells. *J Immunol* **166**, 7571-7578 (2001).
41. Woltmann, G., McNulty, C.A., Dewson, G., Symon, F.A. & Wardlaw, A.J. Interleukin-13 induces PSGL-1/P-selectin-dependent adhesion of eosinophils, but not neutrophils, to human umbilical vein endothelial cells under flow. *Blood* **95**, 3146-3152 (2000).
42. Lum, H. et al. Inflammatory stress increases receptor for lysophosphatidylcholine in human microvascular endothelial cells. *Am J Physiol Heart Circ Physiol* **285**, H1786-1789 (2003).
43. Huang, F., Mehta, D., Predescu, S., Kim, K.S. & Lum, H. A novel lysophospholipid- and pH-sensitive receptor, GPR4, in brain endothelial cells regulates monocyte transmigration. *Endothelium* **14**, 25-34 (2007).
44. Pierrot, C., Beniguel, L., Begue, A. & Khalife, J. Expression of a functional IL-13Ralpha1 by rat B cells. *Biochem Biophys Res Commun* **287**, 969-976 (2001).
45. Zhou, C. et al. The nuclear orphan receptor COUP-TFI is required for differentiation of subplate neurons and guidance of thalamocortical axons. *Neuron* **24**, 847-859 (1999).
46. Mattson, M.P. Neuronal life-and-death signaling, apoptosis, and neurodegenerative disorders. *Antioxid Redox Signal* **8**, 1997-2006 (2006).
47. Davis, M.C. et al. Dexamethasone-induced inositol 1,4,5-trisphosphate receptor elevation in murine lymphoma cells is not required for dexamethasone-mediated calcium elevation and apoptosis. *J Biol Chem* **283**, 10357-10365 (2008).
48. MacKeigan, J.P., Murphy, L.O. & Blenis, J. Sensitized RNAi screen of human kinases and phosphatases identifies new regulators of apoptosis and chemoresistance. *Nat Cell Biol* **7**, 591-600 (2005).
49. Delpire, E. & Mount, D.B. Human and murine phenotypes associated with defects in cation-chloride cotransport. *Annu Rev Physiol* **64**, 803-843 (2002).
50. Schubert, A. & Grimm, S. Cyclophilin D, a component of the permeability transition-pore, is an apoptosis repressor. *Cancer Res* **64**, 85-93 (2004).
51. Hall, C. et al. HIRA, the human homologue of yeast Hir1p and Hir2p, is a novel cyclin-cdk2 substrate whose expression blocks S-phase progression. *Mol Cell Biol* **21**, 1854-1865 (2001).
52. Cao, X., Pfaff, S.L. & Gage, F.H. YAP regulates neural progenitor cell number via the TEA domain transcription factor. *Genes Dev* **22**, 3320-3334 (2008).
53. Overholtzer, M. et al. Transforming properties of YAP, a candidate oncogene on the chromosome 11q22 amplicon. *Proc Natl Acad Sci U S A* **103**, 12405-12410 (2006).
54. Schaffer, B.S., Lin, M.F., Byrd, J.C., Park, J.H. & MacDonald, R.G. Opposing roles for the insulin-like growth factor (IGF)-II and mannose 6-phosphate (Man-6-P) binding activities of the

- IGF-II/Man-6-P receptor in the growth of prostate cancer cells. *Endocrinology* **144**, 955-966 (2003).
55. Souza, R.F. et al. Expression of the wild-type insulin-like growth factor II receptor gene suppresses growth and causes death in colorectal carcinoma cells. *Oncogene* **18**, 4063-4068 (1999).
 56. Bennett, M. et al. Cell surface trafficking of Fas: a rapid mechanism of p53-mediated apoptosis. *Science* **282**, 290-293 (1998).
 57. Osborn, S.L., Sohn, S.J. & Winoto, A. Constitutive phosphorylation mutation in Fas-associated death domain (FADD) results in early cell cycle defects. *J Biol Chem* **282**, 22786-22792 (2007).
 58. Yogosawa, S. et al. Ubiquitylation and degradation of serum-inducible kinase by hVPS18, a RING-H2 type ubiquitin ligase. *J Biol Chem* **280**, 41619-41627 (2005).
 59. Fortschegger, K. et al. Early embryonic lethality of mice lacking the essential protein SNEV. *Mol Cell Biol* **27**, 3123-3130 (2007).
 60. Di Marcotullio, L. et al. REN(KCTD11) is a suppressor of Hedgehog signaling and is deleted in human medulloblastoma. *Proc Natl Acad Sci U S A* **101**, 10833-10838 (2004).
 61. Claude, A. et al. GBF1: A novel Golgi-associated BFA-resistant guanine nucleotide exchange factor that displays specificity for ADP-ribosylation factor 5. *J Cell Biol* **146**, 71-84 (1999).
 62. Gho, J.W. et al. Re-expression of transcription factor ATF5 in hepatocellular carcinoma induces G2-M arrest. *Cancer Res* **68**, 6743-6751 (2008).
 63. Persengiev, S.P., Devireddy, L.R. & Green, M.R. Inhibition of apoptosis by ATFx: a novel role for a member of the ATF/CREB family of mammalian bZIP transcription factors. *Genes Dev* **16**, 1806-1814 (2002).
 64. Aichberger, K.J. et al. Identification of MCL1 as a novel target in neoplastic mast cells in systemic mastocytosis: inhibition of mast cell survival by MCL1 antisense oligonucleotides and synergism with PKC412. *Blood* **109**, 3031-3041 (2007).
 65. Adams, K.W. & Cooper, G.M. Rapid turnover of mcl-1 couples translation to cell survival and apoptosis. *J Biol Chem* **282**, 6192-6200 (2007).
 66. Duckers, H.J. et al. Heme oxygenase-1 protects against vascular constriction and proliferation. *Nat Med* **7**, 693-698 (2001).
 67. Liu, X.M. et al. Endoplasmic reticulum stress stimulates heme oxygenase-1 gene expression in vascular smooth muscle. Role in cell survival. *J Biol Chem* **280**, 872-877 (2005).
 68. Perrotti, D. et al. BCR-ABL prevents c-jun-mediated and proteasome-dependent FUS (TLS) proteolysis through a protein kinase CbetaII-dependent pathway. *Mol Cell Biol* **20**, 6159-6169 (2000).
 69. Hicks, G.G. et al. Fus deficiency in mice results in defective B-lymphocyte development and activation, high levels of chromosomal instability and perinatal death. *Nat Genet* **24**, 175-179 (2000).
 70. Koo, B.H. & Kim, D.S. Factor Xa induces mitogenesis of vascular smooth muscle cells via autocrine production of epiregulin. *J Biol Chem* **278**, 52578-52586 (2003).
 71. Toyoda, H. et al. Epiregulin. A novel epidermal growth factor with mitogenic activity for rat primary hepatocytes. *J Biol Chem* **270**, 7495-7500 (1995).
 72. Hao, Y., Wong, R. & Feig, L.A. RalGDS couples growth factor signaling to Akt activation. *Mol Cell Biol* **28**, 2851-2859 (2008).
 73. Ryu, C.H. et al. The merlin tumor suppressor interacts with Ral guanine nucleotide dissociation stimulator and inhibits its activity. *Oncogene* **24**, 5355-5364 (2005).
 74. Duchene, J. et al. A novel protein-protein interaction between a G protein-coupled receptor and the phosphatase SHP-2 is involved in bradykinin-induced inhibition of cell proliferation. *J Biol Chem* **277**, 40375-40383 (2002).

75. Kakoki, M., McGarrah, R.W., Kim, H.S. & Smithies, O. Bradykinin B1 and B2 receptors both have protective roles in renal ischemia/reperfusion injury. *Proc Natl Acad Sci U S A* **104**, 7576-7581 (2007).
76. Berteaux, N. et al. H19 mRNA-like noncoding RNA promotes breast cancer cell proliferation through positive control by E2F1. *J Biol Chem* **280**, 29625-29636 (2005).
77. Castro, D.S. et al. Induction of cell cycle arrest and morphological differentiation by Nurr1 and retinoids in dopamine MN9D cells. *J Biol Chem* **276**, 43277-43284 (2001).
78. Wallen, A. et al. Fate of mesencephalic AHD2-expressing dopamine progenitor cells in NURR1 mutant mice. *Exp Cell Res* **253**, 737-746 (1999).
79. Moniwa, N., Agata, J., Hagiwara, M., Ura, N. & Shimamoto, K. The role of bradykinin B1 receptor on cardiac remodeling in stroke-prone spontaneously hypertensive rats (SHR-SP). *Biol Chem* **387**, 203-209 (2006).
80. Duchene, J. et al. A novel inflammatory pathway involved in leukocyte recruitment: role for the kinin B1 receptor and the chemokine CXCL5. *J Immunol* **179**, 4849-4856 (2007).
81. Komada, M. & Soriano, P. Hrs, a FYVE finger protein localized to early endosomes, is implicated in vesicular traffic and required for ventral folding morphogenesis. *Genes Dev* **13**, 1475-1485 (1999).
82. Wang, J., Xiao, S.H. & Manley, J.L. Genetic analysis of the SR protein ASF/SF2: interchangeability of RS domains and negative control of splicing. *Genes Dev* **12**, 2222-2233 (1998).
83. Pires, N.M. et al. Activation of nuclear receptor Nur77 by 6-mercaptopurine protects against neointima formation. *Circulation* **115**, 493-500 (2007).
84. Oster, S.K., Ho, C.S., Soucie, E.L. & Penn, L.Z. The myc oncogene: Marvelously Complex. *Adv Cancer Res* **84**, 81-154 (2002).
85. Haxsen, V., Adam-Stitah, S., Ritz, E. & Wagner, J. Retinoids inhibit the actions of angiotensin II on vascular smooth muscle cells. *Circ Res* **88**, 637-644 (2001).
86. Kastner, P. et al. Vitamin A deficiency and mutations of RXRalpha, RXRbeta and RARalpha lead to early differentiation of embryonic ventricular cardiomyocytes. *Development* **124**, 4749-4758 (1997).
87. Toth, R. et al. Activation-induced apoptosis and cell surface expression of Fas (CD95) ligand are reciprocally regulated by retinoic acid receptor alpha and gamma and involve nur77 in T cells. *Eur J Immunol* **31**, 1382-1391 (2001).
88. Hiragun, T., Peng, Z. & Beaven, M.A. Cutting edge: dexamethasone negatively regulates Syk in mast cells by up-regulating SRC-like adaptor protein. *J Immunol* **177**, 2047-2050 (2006).
89. Dragone, L.L., Myers, M.D., White, C., Sosinowski, T. & Weiss, A. SRC-like adaptor protein regulates B cell development and function. *J Immunol* **176**, 335-345 (2006).
90. Singla, D.K. & Sun, B. Transforming growth factor-beta2 enhances differentiation of cardiac myocytes from embryonic stem cells. *Biochem Biophys Res Commun* **332**, 135-141 (2005).
91. Ikedo, H. et al. Smad protein and TGF-beta signaling in vascular smooth muscle cells. *Int J Mol Med* **11**, 645-650 (2003).
92. Bishay, K. et al. DNA damage-related gene expression as biomarkers to assess cellular response after gamma irradiation of a human lymphoblastoid cell line. *Oncogene* **19**, 916-923 (2000).
93. Deng, S. et al. Plexin-B2, but not Plexin-B1, critically modulates neuronal migration and patterning of the developing nervous system in vivo. *J Neurosci* **27**, 6333-6347 (2007).
94. Nicholson, A.C. & Hajjar, D.P. Herpesviruses and thrombosis: activation of coagulation on the endothelium. *Clin Chim Acta* **286**, 23-29 (1999).
95. Ahmad, S.S., Scandura, J.M. & Walsh, P.N. Structural and functional characterization of platelet receptor-mediated factor VIII binding. *J Biol Chem* **275**, 13071-13081 (2000).
96. Saxena, A., Rorie, C.J., Dimitrova, D., Daniely, Y. & Borowiec, J.A. Nucleolin inhibits Hdm2 by multiple pathways leading to p53 stabilization. *Oncogene* **25**, 7274-7288 (2006).

97. Girnita, L. et al. Beta-arrestin and Mdm2 mediate IGF-1 receptor-stimulated ERK activation and cell cycle progression. *J Biol Chem* **282**, 11329-11338 (2007).
98. Ge, L., Shenoy, S.K., Lefkowitz, R.J. & DeFea, K. Constitutive protease-activated receptor-2-mediated migration of MDA MB-231 breast cancer cells requires both beta-arrestin-1 and -2. *J Biol Chem* **279**, 55419-55424 (2004).
99. Van Eynde, A. et al. The nuclear scaffold protein NIPP1 is essential for early embryonic development and cell proliferation. *Mol Cell Biol* **24**, 5863-5874 (2004).
100. Guo, D. et al. Identification and characterization of a novel cytoplasm protein ICF45 that is involved in cell cycle regulation. *J Biol Chem* **279**, 53498-53505 (2004).
101. Ohtsubo, M. et al. Isolation and characterization of the active cDNA of the human cell cycle gene (RCC1) involved in the regulation of onset of chromosome condensation. *Genes Dev* **1**, 585-593 (1987).
102. Chen, D. et al. SKI activates Wnt/beta-catenin signaling in human melanoma. *Cancer Res* **63**, 6626-6634 (2003).
103. Berk, M., Desai, S.Y., Heyman, H.C. & Colmenares, C. Mice lacking the ski proto-oncogene have defects in neurulation, craniofacial, patterning, and skeletal muscle development. *Genes Dev* **11**, 2029-2039 (1997).
104. Henriot, P., Zhong, Z.D., Brooks, P.C., Weinberg, K.I. & DeClerck, Y.A. Contact with fibrillar collagen inhibits melanoma cell proliferation by up-regulating p27KIP1. *Proc Natl Acad Sci U S A* **97**, 10026-10031 (2000).
105. Rossi, D.J. et al. Inability to enter S phase and defective RNA polymerase II CTD phosphorylation in mice lacking Mat1. *EMBO J* **20**, 2844-2856 (2001).
106. Trecia, A. et al. Protein kinase B/Akt binds and phosphorylates PED/PEA-15, stabilizing its antiapoptotic action. *Mol Cell Biol* **23**, 4511-4521 (2003).
107. Sakamoto, S. et al. Increased expression of CYR61, an extracellular matrix signaling protein, in human benign prostatic hyperplasia and its regulation by lysophosphatidic acid. *Endocrinology* **145**, 2929-2940 (2004).
108. Kim, J., Lee, K. & Pelletier, J. The desmoplastic small round cell tumor t(11;22) translocation produces EWS/WT1 isoforms with differing oncogenic properties. *Oncogene* **16**, 1973-1979 (1998).
109. Li, L. et al. PACT is a negative regulator of p53 and essential for cell growth and embryonic development. *Proc Natl Acad Sci U S A* **104**, 7951-7956 (2007).
110. Yan, C. et al. WAVE2 deficiency reveals distinct roles in embryogenesis and Rac-mediated actin-based motility. *EMBO J* **22**, 3602-3612 (2003).
111. Miyata, K. et al. Increase of smooth muscle cell migration and of intimal hyperplasia in mice lacking the alpha/beta hydrolase domain containing 2 gene. *Biochem Biophys Res Commun* **329**, 296-304 (2005).
112. Zhao, H. et al. RECS1 is a negative regulator of matrix metalloproteinase-9 production and aged RECS1 knockout mice are prone to aortic dilation. *Circ J* **70**, 615-624 (2006).
113. Teng, Y., Zeisberg, M. & Kalluri, R. Transcriptional regulation of epithelial-mesenchymal transition. *J Clin Invest* **117**, 304-306 (2007).
114. Niwa, Y. et al. Methylation silencing of SOCS-3 promotes cell growth and migration by enhancing JAK/STAT and FAK signalings in human hepatocellular carcinoma. *Oncogene* **24**, 6406-6417 (2005).
115. Yasukawa, H. et al. Suppressor of cytokine signaling-3 is a biomechanical stress-inducible gene that suppresses gp130-mediated cardiac myocyte hypertrophy and survival pathways. *J Clin Invest* **108**, 1459-1467 (2001).
116. Loughran, G. et al. Mystique is a new insulin-like growth factor-I-regulated PDZ-LIM domain protein that promotes cell attachment and migration and suppresses Anchorage-independent growth. *Mol Biol Cell* **16**, 1811-1822 (2005).

117. Bennett, R.D., Mauer, A.S. & Strehler, E.E. Calmodulin-like protein increases filopodia-dependent cell motility via up-regulation of myosin-10. *J Biol Chem* **282**, 3205-3212 (2007).
118. Sincock, P.M. et al. PETA-3/CD151, a member of the transmembrane 4 superfamily, is localised to the plasma membrane and endocytic system of endothelial cells, associates with multiple integrins and modulates cell function. *J Cell Sci* **112** (Pt 6), 833-844 (1999).
119. Itano, N. et al. Abnormal accumulation of hyaluronan matrix diminishes contact inhibition of cell growth and promotes cell migration. *Proc Natl Acad Sci U S A* **99**, 3609-3614 (2002).
120. Heckman, B.M. et al. Crosstalk between the p190-B RhoGAP and IGF signaling pathways is required for embryonic mammary bud development. *Dev Biol* **309**, 137-149 (2007).
121. McCormick, C., Duncan, G., Goutsos, K.T. & Tufaro, F. The putative tumor suppressors EXT1 and EXT2 form a stable complex that accumulates in the Golgi apparatus and catalyzes the synthesis of heparan sulfate. *Proc Natl Acad Sci U S A* **97**, 668-673 (2000).
122. Fehrenbacher, N. et al. Sensitization to the lysosomal cell death pathway by oncogene-induced down-regulation of lysosome-associated membrane proteins 1 and 2. *Cancer Res* **68**, 6623-6633 (2008).
123. Prasad, D.V. et al. The Th1-specific costimulatory molecule, m150, is a posttranslational isoform of lysosome-associated membrane protein-1. *J Immunol* **169**, 1801-1809 (2002).
124. Chauhan, A.K. et al. Systemic antithrombotic effects of ADAMTS13. *J Exp Med* **203**, 767-776 (2006).
125. Kim, Y.S. et al. Kruppel-like zinc finger protein Glis2 is essential for the maintenance of normal renal functions. *Mol Cell Biol* **28**, 2358-2367 (2008).
126. Nanda, N. et al. Platelet endothelial aggregation receptor 1 (PEAR1), a novel epidermal growth factor repeat-containing transmembrane receptor, participates in platelet contact-induced activation. *J Biol Chem* **280**, 24680-24689 (2005).
127. Duke-Cohan, J.S. et al. Attractin (DPPT-L), a member of the CUB family of cell adhesion and guidance proteins, is secreted by activated human T lymphocytes and modulates immune cell interactions. *Proc Natl Acad Sci U S A* **95**, 11336-11341 (1998).
128. Li, X. et al. CHST1 and CHST2 sulfotransferase expression by vascular endothelial cells regulates shear-resistant leukocyte rolling via L-selectin. *J Leukoc Biol* **69**, 565-574 (2001).
129. Gomez-Cambronero, J., Horn, J., Paul, C.C. & Baumann, M.A. Granulocyte-macrophage colony-stimulating factor is a chemoattractant cytokine for human neutrophils: involvement of the ribosomal p70 S6 kinase signaling pathway. *J Immunol* **171**, 6846-6855 (2003).
130. Lee, T.C., Ho, I.C., Lu, W.J. & Huang, J.D. Enhanced expression of multidrug resistance-associated protein 2 and reduced expression of aquaglyceroporin 3 in an arsenic-resistant human cell line. *J Biol Chem* **281**, 18401-18407 (2006).
131. Li, Z., Shi, H.Y. & Zhang, M. Targeted expression of maspin in tumor vasculatures induces endothelial cell apoptosis. *Oncogene* **24**, 2008-2019 (2005).
132. Tadros, A., Hughes, D.P., Dunmore, B.J. & Brindle, N.P. ABIN-2 protects endothelial cells from death and has a role in the antiapoptotic effect of angiopoietin-1. *Blood* **102**, 4407-4409 (2003).
133. Borrell-Pages, M. et al. Cystamine and cysteamine increase brain levels of BDNF in Huntington disease via HSJ1b and transglutaminase. *J Clin Invest* **116**, 1410-1424 (2006).
134. Lin, K.R. et al. Survival factor withdrawal-induced apoptosis of TF-1 cells involves a TRB2-Mcl-1 axis-dependent pathway. *J Biol Chem* **282**, 21962-21972 (2007).
135. Nakano, K. & Vousden, K.H. PUMA, a novel proapoptotic gene, is induced by p53. *Mol Cell* **7**, 683-694 (2001).
136. Liu, L., Sakai, T., Sano, N. & Fukui, K. Nucling mediates apoptosis by inhibiting expression of galectin-3 through interference with nuclear factor kappaB signalling. *Biochem J* **380**, 31-41 (2004).
137. Kaminker, P.G. et al. TANK2, a new TRF1-associated poly(ADP-ribose) polymerase, causes rapid induction of cell death upon overexpression. *J Biol Chem* **276**, 35891-35899 (2001).

138. Albayrak, T. et al. The tumor suppressor cybL, a component of the respiratory chain, mediates apoptosis induction. *Mol Biol Cell* **14**, 3082-3096 (2003).